ACCOUNTS
of chemical research

Selective Localization of Preformed Nanoparticles in Morphologically Controllable Block Copolymer Aggregates in Solution

YIYONG MAI AND ADI EISENBERG*
Department of Chemistry, McGill University, 801 Sherbrooke Street West, Montreal, Quebec H3A 2K6, Canada

RECEIVED ON DECEMBER 2, 2011

CONSPECTUS

The development of nanodevices currently requires the formation of morphologically controlled or highly ordered arrays of metal, semiconducting, or magnetic nanoparticles. In this context, polymer self-assembly provides a powerful bottom-up approach for constructing these materials. The self-assembly of block copolymers (BCPs) in solution is a facile and popular method for the preparation of aggregates of controllable morphologies, including spherical micelles, cylindrical micelles, vesicles (or polymersomes), thin films, and other complex structures that range from zero to three dimensions. Researchers can generally control the morphology of the aggregates by varying copolymer composition or environmental parameters, including the copolymer concentration, the common solvent, the content of the precipitant, or the presence of additives such as ions, among others. For example, as the content of the hydrophilic block in amphiphilic copolymers decreases, the aggregates formed from the copolymers can change from spherical micelles to cylindrical micelles and to vesicles. The aggregates of various morphologies provide excellent templates for the organization of the nanoparticles.

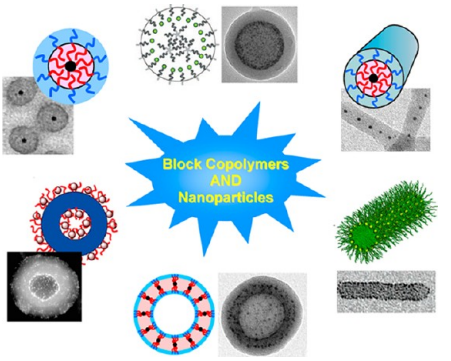

The presence of various domains, such as cores, interfaces, and coronas, in BCP aggregates allows for selective localization of nanoparticles in different regions, which may critically affect the resulting properties and applications of the nanoparticles. For example, the incorporation of quantum dots (QDs) into micelle cores solves many problems encountered in the utilization of QDs in biological environments, including enhancement of water solubility, aggregation prevention, increases in circulation or retention time, and toxicity clearance. Simultaneously it preserves the unique optical performance of QDs compared with those of organic fluorophores, such as size-tunable light emission, improved signal brightness, resistance against photobleaching, and simultaneous excitation of multiple fluorescence colors. Therefore, many studies have focused on the selective localization of nanoparticles in BCP aggregates.

This Account describes the selective localization of preformed spherical nanoparticles in different domains of BCP aggregates of controllable morphologies in solution, including spherical micelles, cylindrical micelles, and vesicles. These structures offer many potential applications in biotechnology, biomedicine, catalysis, etc. We also introduce other types of control, including interparticle spacing, particle number density, or aggregate size control. We highlight examples in which the surface coating, volume fraction, or size of the particles was tailored to precisely control incorporation. These examples build on the thermodynamic considerations of particle–polymer interactions, such as hydrophobic interactions, hydrogen bonding, electrostatic interactions, and ligand replacement, among others.

1. Introduction

Block copolymer (BCP) aggregates of controllable morphologies provide excellent templates for organization of metal, semiconducting, or magnetic nanoparticles (NPs).[1−6] Selective localization of the NPs in different domains of BCP aggregates of various morphologies may critically affect their resulting properties and possible applications. Two primary approaches have been employed for incorporation of NPs into BCP aggregates. The first adopts *in situ* NP synthesis; that is, metal ions are bound or adsorbed into

Published on the Web 07/30/2012 www.pubs.acs.org/accounts
10.1021/ar2003144

BCP aggregates, followed by postassembly chemical reactions to transform the metal ions into NPs. This method has been reviewed in a number of papers.[1,2,5,6] A typical example involves the embedding of NPs into polystyrene-*block*-polyvinylpyridine (PS-*b*-PVP) aggregates.[2,5] However, this method is not suitable for preformed NPs or aggregates made of BCPs incapable of binding, adsorbing, or otherwise incorporating metal ions. Besides, the NPs are limited to the metal ion binding or adsorbing regions of the BCP aggregates. The second approach involves *ex situ* NP preparation, in which the NPs are preformed and stabilized with organic chains on the surfaces, followed by the co-self-assembly of the NPs and BCPs, or the self-assembly involving the NPs alone. This method does not require postassembly chemical reactions within the aggregates and is thus expected to be suitable for a wide range of NPs and BCP systems. Furthermore, surface modification of preformed NPs makes them compatible with specific segments of BCPs, offering an opportunity for position control of the NPs in different regions of the BCP aggregates or even in different parts of the same domain of the aggregates.

This Account reviews the selective localization of preformed spherical NPs in BCP spherical micelles, cylindrical micelles, and vesicles in solution, which have great potential applications in, among others, biotechnology, biomedicine, and catalysis.[7] Due to space limitations, this Account will not discuss particle incorporation into bulk, thin films, or other complex structures, since reviews exist covering these aspects,[2−5] nor will it review *in situ* particle incorporation or aggregates made of BCP systems other than linear BCPs.

2. Spherical Micelles

Spherical micelles, which consist of a spherical core and a corona,[7] can contain a wide ranging number of NPs after incorporation. Micelles containing a single NP are frequently referred to as "cherry micelles" and micelles containing multiple NPs as "raspberry micelles". Paralleling the core−corona structure of the micelles, the order of presentation to be followed in this section regarding the localization control will be core−interface−corona, which will also be followed in the subsequent sections for cylindrical micelles and vesicles.

2.1. Cherry Micelles. Two *ex situ* strategies are employed to prepare cherry micelles. One is chemically anchoring organic chains on the particle surfaces, through, for example, the well-known Brust−Schiffrin synthesis[8] or Murray's place-exchange technique.[9] Typical examples include attachment of functionalized polymers to surfaces, polymerization from particle-bound initiators, layer-by-layer deposition, or synthesis of NPs in the presence of polymeric ligands.[8−10] This approach limits NPs to the middle of the micelles, and thus represents central localization control. However, this method is unlikely to localize NPs in other portions of the micelles, such as at the interfaces or in the coronas. The other strategy, which is the focus of this subsection, is co-self-assembly of preformed NPs and BCPs. This method provides opportunities to achieve selective localization of NPs by tailoring their surface coating or their size.

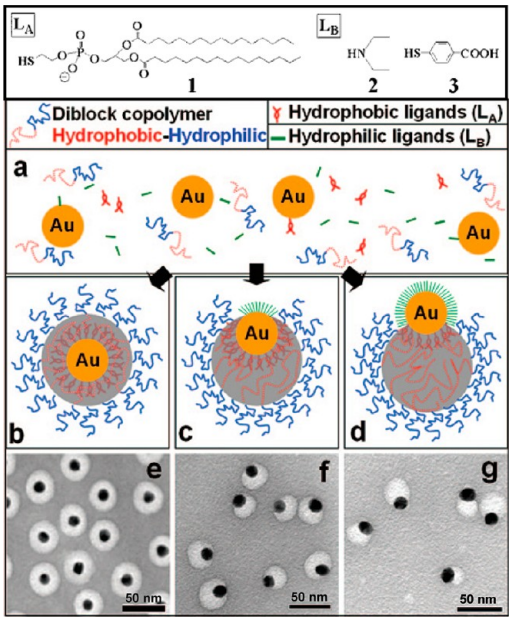

FIGURE 1. Schematic diagrams of the formation of cherry micelles with selective particle localization from the center (a, b) to the interface (a, c or a, d), and the corresponding TEM images when [**1**]/[**2**] = 1:0 (e); 1:22 (f); 1:132 (g).[11]

An excellent introductory example of particle localization control in cherry micelles is a study from Chen's group,[11] although central localization had been reported earlier.[12−15] Figure 1 shows the schematic position control of the particles in micelles along with the corresponding TEM images. The control was accomplished by virtue of a binding competition between a hydrophobic ligand (L_A, see Figure 1) and a hydrophilic one (L_B, Figure 1) on the surface of the gold NPs (AuNPs), which leads to selective adsorption of amphiphilic polystyrene-*block*-poly(acrylic acid) (PS-*b*-PAA) chains on the L_A attached side of the AuNPs, and consequently the selective localization of the particles in the micelles in positions from the center to the interface. The studies were performed by a "mix-and-heat" approach; that is, a mixture of AuNPs, PS-*b*-PAA, L_A, with or without L_B in DMF/H_2O (4:1, v/v) was heated at 110 °C for 2 h and then slowly

cooled to form the micelles. By this means, a single AuNP of 5−15 nm diameter was encapsulated into each micelle.[11,15] The proposed mechanism suggests that the particle provides a surface template for the hydrophobic interaction-driven adsorption of polymer chains.

Some studies elucidated the influence of particle size on the number of encapsulated particles. Kang and Taton[13,14] encapsulated a single AuNP into the PS core of each PS-*b*-PAA micelle when the AuNPs were larger than 10 nm, by adding water into DMF solutions of citrate-capped AuNPs, dodecanethiol, and PS-*b*-PAA copolymers. For smaller AuNPs (~4 nm diameter), multiple particles were encapsulated in each micelle, even at very low particle-to-polymer ratios.[13] It was suggested that for small NPs ($R_{Au}/R_g \leq 1$, where R_{Au} is the radius of the AuNPs and R_g is the radius of gyration of the polymer chains), particles behave like solutes dissolved within micelle cores, presumably to maximize their entropy; for larger NPs ($R_{Au}/R_g > 1$), polymer chain adsorption is templated by the particle surface, leading to the encapsulation of a single particle and the formation of a concentric polymer shell around the particle. The thickness of the shell increased with increasing PS block length or ratio of polymer to available particle surface area.[14] However, this conclusion is inapplicable to some other large NPs (>10 nm), for example, Fe_2O_3 NPs. In those cases, only micelles with multiple core-embedded NPs could be obtained, even at very low particle-to-polymer ratios, as shown in a subsequent study (ref 22, to be discussed in the Raspberry Micelles subsection).

A new method was recently developed to incorporate preformed NPs into only the center of micelles.[16] The method involves stabilizing the NPs with diblock copolymers of a similar composition to that of the micelle-forming diblocks, followed by preparing the micelles in the presence of the copolymer-coated NPs in solution. Figure 2 shows a TEM image of the cherry micelles along with a model in which the hydrophilic or hydrophobic blocks of the diblock chains on the particle surface aggregate together with the corresponding unattached hydrophilic or hydrophobic segments of the micelle-forming diblocks. This approach forces the NPs to localize near the center of the micelles, which avoids a large energy induced by the asymmetric stretching of polymer chains on the noncentrally localized NPs. Utilizing this method, encapsulation of multiple NPs in a single micelle becomes highly unlikely, even for small NPs.

To our knowledge, cherry micelles with corona-located NPs have not been reported yet.

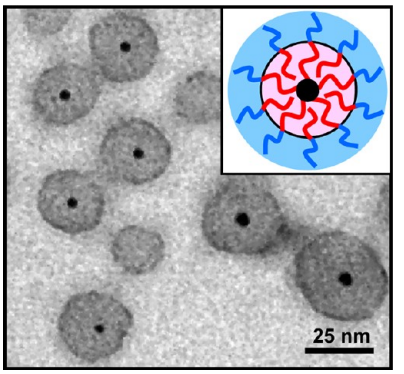

FIGURE 2. TEM image and schematic diagram (inset) of cherry micelles with core-centric AuNPs formed by coassembly of PS-*b*-PAA diblocks (unanchored chains in the diagram) and PS-*b*-PAA coated AuNPs.[16] Red, PS segments in micelle core; blue, PAA segments in corona.

2.2. Raspberry Micelles **2.2.1. Particles in Cores.** There are two popular strategies to embed multiple NPs in micelle cores. One is the polymer-mediated "bricks and mortar" strategy; the other is the "hydrophobic interaction-driven microphase separation" strategy.

The "bricks and mortar" strategy was developed by Rotello and co-workers. In one of their studies,[17] a diblock copolymer with the first block of polystyrene and the second block of a random copolymer of styrene and diaminotriazine-functionalized styrene was prepared as the "mortar". Thymine-functionalized AuNPs were employed as the "bricks" (Figure 3a). Aggregation of the mortar and the bricks in solution produced micellar aggregates with multiple AuNPs in the cores through hydrogen bonding between the diaminotriazine groups in the copolymer and the thymine groups on the particle surfaces. The average size of the cores of the micelles can be controlled by adjusting the block length of the copolymer (Figure 3b). This strategy provides an effective route to organize NPs together with BCPs and control the sizes of the aggregates. Subsequently, this strategy was also adopted to control the clustering of NPs by electrostatic coassembly of oppositely charged NPs and BCPs.[18]

A typical procedure for the "hydrophobic interaction-driven microphase separation" approach involves dissolution of NPs and amphiphilic copolymers in a common solvent, in which the NPs and the copolymers are soluble, followed by addition of a selective solvent. The selective solvent simultaneously desolvates the NPs and the hydrophobic polymer blocks, leading to the aggregation of the NPs with the hydrophobic blocks, forming hydrophobic parts of the aggregates, for example, micelle cores, which are protected by the hydrophilic segments. This process

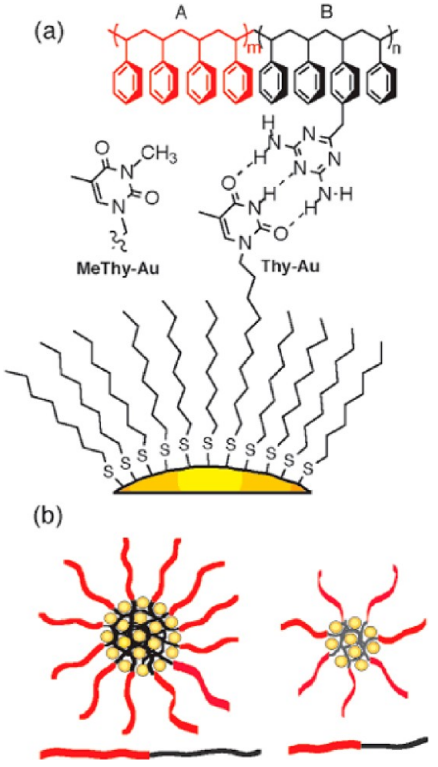

FIGURE 3. (a) An example of the "bricks and mortar" strategy to organize particles together with BCPs. (b) Schematic demonstrating an increase in both core diameter and outer corona as the polymer size increases.[17]

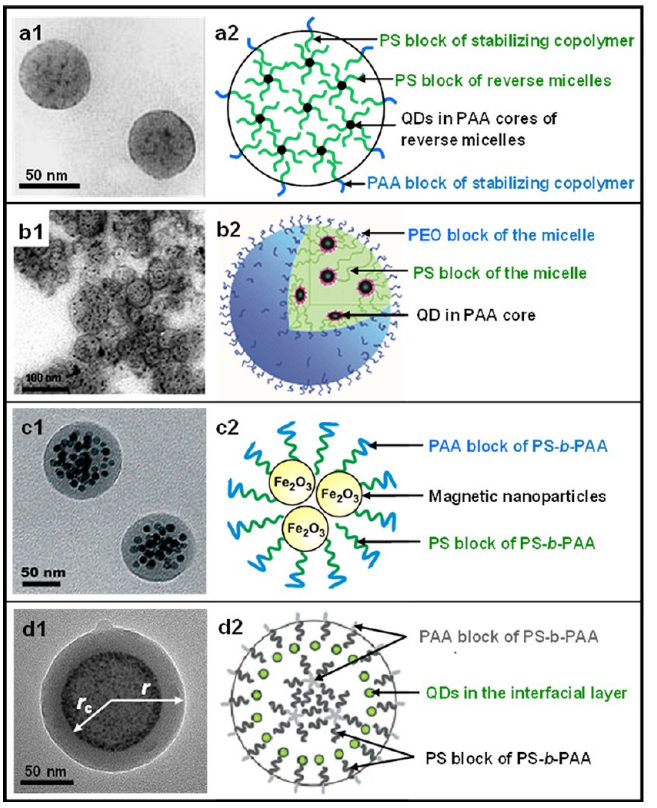

FIGURE 4. TEM images and the corresponding schematic diagrams of different types of micellar aggregates with core-encapsulated nanoparticles: (a) large compound micelles;[19] (b) supermicelles;[21] (c) magnetomicelles;[22] (d) a micellar aggregate with QDs located at a radial position (r_c/r) in the core.[25] Reproduced with permission from ref 25, copyright 2007, John Wiley & Sons, Inc.

sacrifices the entropy term but prevents a larger enthalpy penalty from energetically unfavorable hydrophobe–water interactions and therefore lowers the free energy of the system. Several types of micelles containing core-encapsulated NPs were prepared by this method, including large compound micelles (LCMs), supermicelles, etc.

LCMs consist of assemblies of reverse micelles stabilized in solution by a thin layer of hydrophilic chains. Moffitt et al.[19] reported the synthesis of CdS quantum dots (QDs) within the PAA cores of PS-*b*-PAA reverse micelles. The aggregation of these reverse micelles with a stabilizing copolymer (another PS-*b*-PAA copolymer) produced LCMs with QDs dispersed throughout a spherical PS matrix, which was stabilized in water by a layer of hydrophilic PAA chains from the stabilizing diblocks (Figure 4a). The LCMs had a narrowly distributed diameter of ~64 nm, and the average interparticle distance within the LCM was calculated to be 12 nm. Since the interparticle spacing is mainly governed by the bulk volume of the reverse micelle corona, it can be easily tuned by using reverse micelles with different PS block lengths. Besides, the average LCM size can be increased by increasing the initial concentration of the stabilizing copolymer or decreasing the rate of water addition.[20]

QD-containing supermicelles composed of poly(acrylic acid)-*block*-polystyrene-*block*-poly(ethylene oxide) (PAA-*b*-PS-*b*-PEO) are shown in Figure 4b.[21] These supermicelles were obtained by an accretion of spherical micelles with a QD-loaded PAA core and a PS-*b*-PEO corona, which was induced by interactions of the hydrophobic PS chains as the water content increased, leaving the hydrophilic PEO chains outside the supermicelles as coronas. In the supermicelles, each of the PS chains is linked at one end to the outer surface of the supermicelles via the PEO chain and at the other end via the PAA chain to one of the QDs. The PS chains span the distance between the QDs and the interface of the supermicelle. The QD size can be controlled by the PAA block length, and the total diameter of the supermicelles is a function of the PS block length.

Another type of micellar aggregate with core-embedded NPs is formed by coassembly in solution of amphiphilic BCPs and NPs stabilized with small-molecule surfactants. For instance, Taton and co-workers[22] prepared "magnetomicelles" (Figure 4c) by adding water into DMF/THF solutions

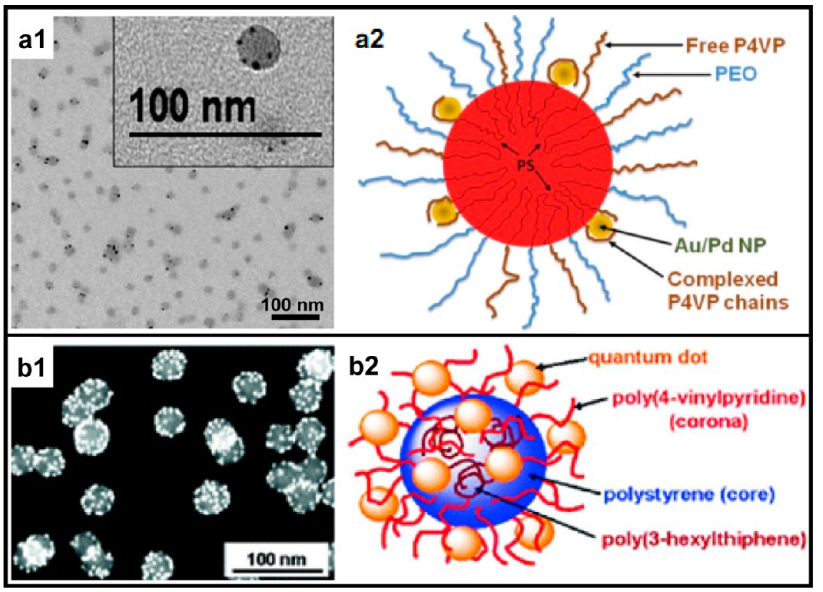

FIGURE 5. TEM images and the corresponding schematic diagrams of micelles with nanoparticles located at the interface between the core and the corona (a)[27] or in the corona (b).[29]

of oleic acid-coated magnetic NPs and PS-*b*-PAA. The NPs act like solutes dissolved within the micelle cores. The average number of encapsulated NPs in each micelle increases as the particle-to-polymer ratio increases, while the distribution of NPs in micelles in each sample is roughly Gaussian. The size of the magnetomicelles increases linearly with the number of embedded NPs. This represents an effective aggregate size control technique. Building on similar mechanisms, a number of other studies were reported, dealing with the preparation of micelles with core-located NPs;[23] they are not described here because of space limitations.

A simulation of the self-assembly of BCP/NP mixtures in solution, based on self-consistent-field and density-functional theories, shows that with small volume fractions or sizes the particles would favor a random distribution in micelle core, while with larger volume fractions or sizes the particles would prefer an interfacial localization driven by unfavorable mixing energies, for example, from steric packing.[24]

Some experimental results support the simulation of interfacial localization. Park's group[25,26] reported a unique type of micellar aggregate, which consists of an outer polymer shell, an inner polymer core, and QDs selectively arranged in a spherical layer at the interface between the core and the shell (Figure 4d). The aggregates were prepared by addition of water into DMF solutions of trioctylphosphine oxide (TOPO) stabilized QDs and PS-*b*-PAA copolymers. The slightly unfavorable interaction between the PS segment of the copolymers and the alkyl-coated QDs causes the interfacial accumulation of the QDs, which reduces the polymer stretching penalty that would occur by incorporating the QDs throughout the polymer matrix. The size of the micelles and the radial position (r_c/r) of the QDs are controlled by varying the QD volume fraction (Φ_{QD}). At a fixed QD size, the increase in Φ_{QD} results in a decrease in the average micelle size and an increase in r_c/r over a wide range of Φ_{QD}. These experimental results qualitatively match the strong segregation theory calculations.[26]

2.2.2. Particles at Interfaces. The primary approach to achieve precise localization of NPs at the micellar interface utilizes triblock copolymers as self-assembly precursors; one of the blocks is selected to interact with the NPs, while the other forms either the core or the corona of micelles. Azzam et al.[27] prepared a triblock copolymer of PEO-*b*-PS-*b*-P4VP. Coassembly of this copolymer with tetraoctylammonium bromide (TOAB) stabilized Au or Pd NPs in solution produced micelles with the NPs located at the interface between the PS core and the PEO corona (Figure 5a). The interfacial localization of the NPs is attributed to the difference in the hydrophobic nature of PS and P4VP blocks. PS blocks, which are more hydrophobic than P4VP blocks, aggregate first and form the core during the self-assembly accompanying water addition. Subsequently, the P4VP blocks, which are associated with the NPs after replacing the TOAB ligands, form a shell containing both the NPs and the P4VP blocks on the PS core. Recently, Moffitt's group[28] prepared CdS QDs surrounded by mixed brushes of hydrophobic PS and hydrophilic poly(methacrylic acid) (PMAA). The synthesis started with cross-linking the PAA blocks of PS-*b*-PAA-*b*-PMMA

triblocks with Cd^{2+}, followed by the reaction with H_2S and hydrolysis of poly(methyl methacrylate) (PMMA) to PMAA. Addition of water into THF solution of these NPs generated large micelles, in which the PS and the PMAA brushes formed the cores and the coronas, respectively, leaving the QDs at the interfaces.

2.2.3. Particles in Coronas. Localization of preformed NPs in micelle coronas is driven by corona−particle interactions. Winnik and co-workers[29] prepared PS-*b*-P4VP micelles containing QDs in the P4VP corona and poly(3-hexylthiophenes) in the PS core (Figure 5b), by addition of alcohol into chloroform solutions of TOPO-coated QDs, poly(3-hexylthiophenes), and PS-*b*-P4VP. Ligand replacement of the TOPO by the P4VP blocks allowed the coronal incorporation of the QDs. The excited-state photoluminescence quenching of the QDs by poly(3-hexylthiophenes) in the core indicated electronic energy transfer or photoinduced charge transfer between the QDs and the conducting polymer. This system provides a model for studies of blended photovoltaic materials with spatially organized components. An alternative method utilizes biomolecule-mediated particle−corona binding. For example, AuNPs coated with single-stranded DNA could be tethered to micelle coronas functionalized with cDNA sequences.[30]

3. Cylindrical Micelles

Cylindrical micelles, which consist of a cylindrical core surrounded by coronal chains, are generally the next aggregates after spherical micelles in morphological transitions as copolymer composition or environmental parameters are adjusted.[7] Precise incorporation of NPs into different regions of cylindrical micelles plays a crucial role in construction of one-dimensional nanostructures of NPs, which have attracted great interest owing to their potential applications in new optoelectronic or microelectronic devices.[6]

3.1. Particles in Cores. Several studies achieved the random localization of preformed NPs in the cores of cylindrical micelles.[21,31−33] The precise incorporation of preformed NPs into only the central portion of cylindrical micelles has been reported only recently.[16,34] Mai and Eisenberg[16] achieved such localization of AuNPs in the PS core of PS-*b*-PAA rod-like aggregates (Figure 6a), based on coating the NPs with amphiphilic copolymers of a similar composition to that of the rod-forming diblocks. The schematic model is shown in Figure 6a2. The explanation is similar to that given previously for the model in Figure 2 and is not repeated here. Using this method, the central

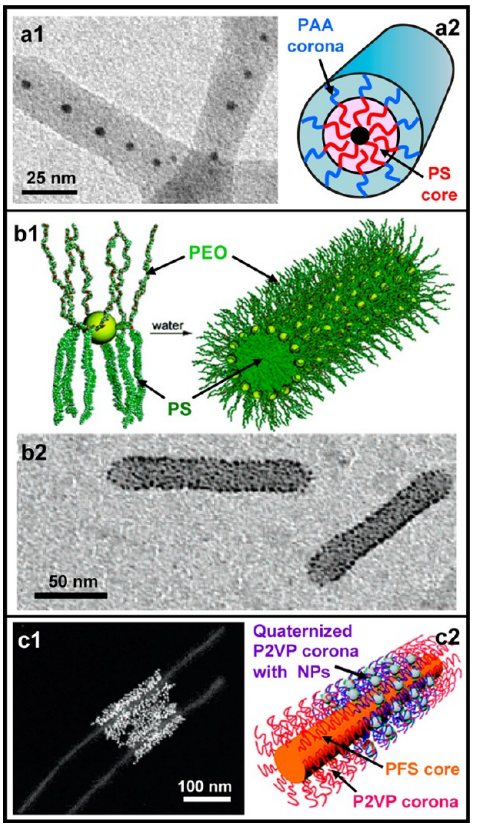

FIGURE 6. TEM images and the corresponding schematic diagrams of cylindrical micelles with nanoparticles precisely localized in the middle of the core (a),[16] at the interface between the core and the corona (b),[35] or in a part of the corona (c).[37] In a2, the rod-forming diblocks are unanchored on the particle, which have a similar composition to the diblocks anchored on the particle.

localization becomes independent of weight ratio of NPs to rod-forming copolymers. The average distance between adjacent NPs along the rods is readily controlled by adjusting the weight ratio; the larger the ratio, the smaller the interparticle distance.

Li et al.[34] reported the localization of homo-PS coated AuNPs along the centerline of the PS core of PS-*b*-P4VP wormlike micelles. The central localization of the AuNPs in the compatible PS domain sacrifices the localization entropy of the NPs but avoids an even larger penalty caused by the deformation of polymer chains surrounding the noncentrally located NPs. In this case, the mean interparticle distance also decreases with increasing particle-to-polymer ratio, leading to a red-shift of the surface plasmon resonance spectrum of the hybrid cylindrical micelles. This central localization shows a dependence on particle size. At a same volume fraction, small AuNPs ($D/R_0 < 1$, where D is the diameter of the PS-coated AuNPs and R_0 is the root-mean-square end-to-end distance of PS block) prefer a random

distribution within the micelle cores to maximize their entropy because of the larger translational entropy than that of large NPs.

3.2. Particles at Interfaces. Precise localization of NPs at the interfaces of cylindrical micelles can produce tubular NP arrays. Two approaches were developed for the interfacial incorporation. One is binding a NP to a junction point of an amphiphile, followed by self-assembly of the modified NPs. Zubarev et al.[35] synthesized PS-*b*-PEO diblocks containing a carboxylic group at the junction point and attached them to phenol-functionalized gold or silver NPs (Figure 6b). Self-assembly of the copolymer-coated NPs in solution generated cylindrical micelles with NPs located at the interface between the PS core and the PEO corona. The other method uses triblock copolymers as self-assembly precursors, in which one block interacts with the NPs, while the other two form the core and the corona, respectively. Winnik and co-workers[36] prepared wormlike micelles using PS-*b*-P4VP-*b*-PEO triblocks, and incorporated TOPO-capped QDs into the interfacial P4VP layer between the PS core and the PEO corona, through replacing the TOPO ligands with the P4VP blocks.

3.3. Particles in Coronas. The particle–corona interactions, for example, electrostatic attraction,[37,38] can bind preformed NPs to the coronas of cylindrical micelles. An illustrative example is given in Figure 6c, which shows the localization of NPs in the quaternized P2VP coronas of cylindrical micelles of polyferrocenylsilane-*b*-poly(2-vinylpyridine) (PFS-*b*-P2VP).[37] The cylindrical micelles were generated by living self-assembly, in which PFS-*b*-P2VP assembled at both ends of the quaternized micelles driven by epitaxial crystallization of PFS blocks. Selective localization of the particles was accomplished by electrostatically driven deposition of AuNPs or PbS QDs coated with negatively charged ligands on the positively charged vinylpyridine fragments.

3.4. Particles in Other Locations. Wooley, Pochan, and co-workers[39] prepared wormlike aggregates with periodic transversal PAA layers by self-organization of amphiphilic poly(acrylic acid)-*block*-poly(methyl acrylate)-*block*-polystyrene (PAA-*b*-PMA-*b*-PS) along with organic diamines in THF/water solution (Figure 7). Amine-functionalized AuNPs were then incorporated into the PAA layers driven by electrostatic attraction, forming AuNP stripes periodically distributed along the aggregates. Moffitt and co-workers[28] obtained an analogous wormlike nanostructure, by self-assembly of CdS QDs surrounded by mixed brushes of hydrophobic PS and hydrophilic PMAA also in THF/water solution; alternating transverse layers of PS and QDs dispersed within PMAA were observed in this nanostructure.

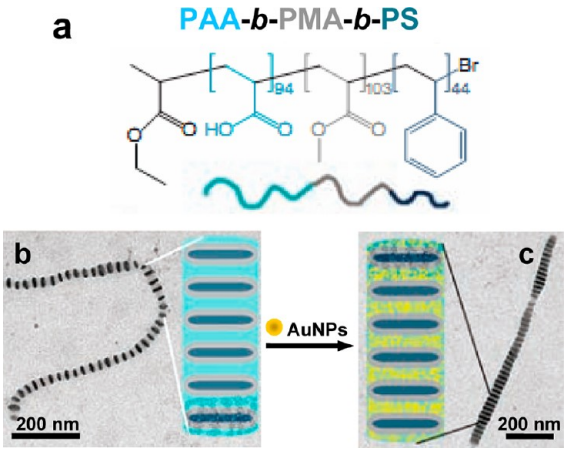

FIGURE 7. Selective localization of cationic AuNPs in the negatively charged PAA regions of the striped wormlike aggregates formed from a PAA-*b*-PMA-*b*-PS copolymer.[39] Reproduced with permission from ref 39, copyright 2007, The American Association for the Advancement of Science.

4. Vesicles

Vesicles are usually hollow spheres with a hydrophobic wall and hydrophilic internal and external coronas, which represent the next step in the arrangement of BCP chains after cylindrical micelles as copolymer composition or environmental parameters change.[7] They provide excellent templates for organization of NPs into three-dimensional hollow spherical structures through selective incorporation of NPs into their walls, interfaces, or coronas.

4.1. Particles in Vesicle Walls. Incorporation of particles into vesicle walls may open up applications for vesicles that call for simultaneous encapsulation of hydrophobic NPs, for example, labeled or catalytic species, into vesicle walls, along with hydrophilic species into cavities. A common method for the incorporation employs coassembly in solution of amphiphilic BCPs and the NPs coated with small-molecule surfactants. Driven by hydrophobic interactions, the NPs and the hydrophobic polymer segments aggregate into vesicle walls, leaving the hydrophilic blocks as coronas. Through this approach, Lecommandoux and co-workers[40] obtained vesicle-like membranes with NPs randomly distributed inside by coassembly of polybutadiene-*block*-poly(glutamic acid) (PB-*b*-PGA) copolymers and Fe_2O_3 NPs stabilized with a phosphoric diester surfactant. Afterward, additional well-defined vesicular structures with preformed NPs located randomly in the walls were reported.[41–44]

Recently, Mai and Eisenberg[45] reported a general approach for controlled incorporation of preformed NPs into

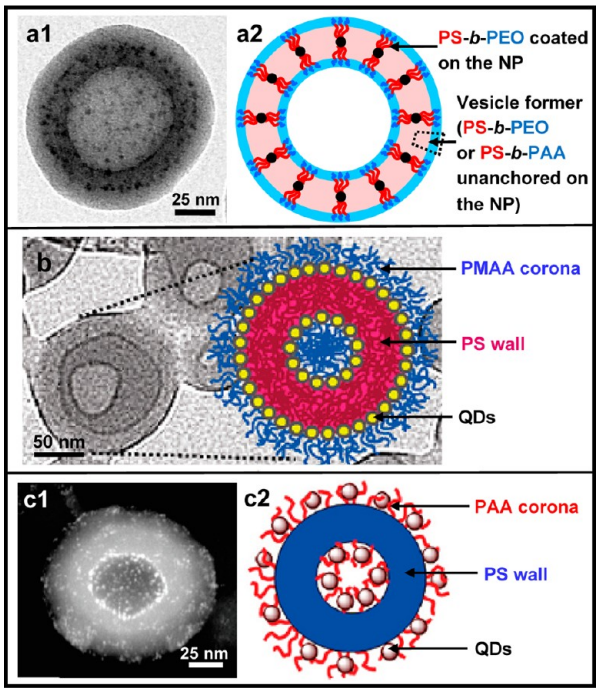

FIGURE 8. TEM images and the corresponding schematic diagrams of vesicles with nanoparticles precisely localized in the middle of the wall (a),[45] at the interfaces between the wall and the coronas (b),[28] or in the coronas (c).[48]

only the central portion of vesicle walls, based on stabilizing the NPs with amphiphilic copolymers of the same or similar composition as that of the vesicle-forming diblocks. Figure 8a1 shows a TEM image of the vesicles with Pb NPs in the middle portion of the wall. Figure 8a2 presents a schematic illustration of the wall incorporation, in which each NP is located at the center of the wall, with the corona chains extended more or less equally toward each interface. The aggregates in the wall are drawn with the hydrophilic segments of the protective diblocks in the water phase, along with the hydrophilic segments of the vesicle-forming diblocks. This symmetric way would force NPs to localize near the wall center, in order to reduce the high free energy associated with the asymmetric distribution and stretching of polymer chains on the noncentrally localized NPs. By this means, the central localization is independent of particle-to-polymer ratio, as demonstrated experimentally.

Subsequently, Park's group[46] achieved the dense packing of oleic acid-coated magnetic NPs in the middle of the PS walls of PS-*b*-PAA vesicles. The small bulk volume of the small-molecule coating facilitates the dense particle packing. At high particle-to-copolymer ratios, the NPs prefer a random localization in the wall, in order to reduce the steric packing energy caused by central localization and to maximize the entropy. By controlling the solvent–particle or polymer–particle interactions, this study achieved additionally the random or interfacial distribution of the magnetic NPs in PS-*b*-PAA micelles and thus represents an example of selective localization of NPs in morphologically controllable aggregates from micelles to vesicles.

A special case, in which amphiphilic QDs make up vesicles directly, was reported by Förster and co-workers.[47] They coated CdSe/CdS QDs with poly(ethylene oxide)-*block*-branched polyethyleneimine (PEO-PEI) through ligand replacement; self-assembly of such NPs with a low copolymer coating density in solution produced vesicles with walls consisting of a monolayer of the QDs.

4.2. Particles at Interfaces. Through the strategy described previously for the interfacial localization of preformed NPs in raspberry micelles, that is, by self-assembly of the QDs surrounded by mixed brushes of PS and PMAA, Moffitt's group[28] obtained vesicles in which the PS brushes form the walls while the PMAA constructs the coronas, leaving the QDs at both internal and external interfaces (Figure 8b).

4.3. Particles in Coronas. The particle–corona interactions, again, play a key role in particle incorporation into vesicle coronas. Winnik and co-workers[48] incorporated oleic acid-capped NPs or TOPO-coated QDs into the PAA coronas of PS-*b*-PAA vesicles (Figure 8c), by adding water into THF/dioxane solutions of the NPs and PS-*b*-PAA. The binding of the PAA block to the particle surfaces and the subsequent ligand replacement led to the coronal localization of the NPs. Opsteen et al.[49] "clicked" biotin to the coronas of PS-*b*-PAA vesicles and then treated them with streptavidin-modified AuNPs; the strong affinity of biotin and streptavidin enabled the binding of the AuNPs to the external corona of the vesicles. A different mechanism involves a micelle–vesicle transformation. Hou et al.[50] prepared hybrid PS-*b*-P4VP micelles with PS coronas and AuNPs in protonated P4VP cores in chloroform. After switching the solvent gradually from chloroform to a methanol/chloroform mixture, in which the protonated P4VP is soluble while PS is insoluble, a core–corona inversion of the micelles occurred, forming vesicles with PS walls and the AuNPs located in the protonated P4VP coronas. The AuNPs could be released by deprotonating the P4VP coronas. This study provides a new strategy for particle encapsulation and release in organic solutions.

5. Summary/Outlook

This Account describes the selective localization of preformed NPs in BCP spherical micelles, cylindrical micelles,

and vesicles. The morphology of the aggregates can generally be controlled through adjusting copolymer composition and concentration, nature of the common solvent, content of precipitant, presence of additives, etc. Examples are highlighted in which the surface coating, volume fraction, or size of the NPs was tailored to achieve precisely controlled incorporation, building on considerations of enthalpic and entropic particle–polymer interactions, including hydrophobic interaction, hydrogen bonding, ligand replacement, and electrostatic interaction, among others.

Controlled particle incorporation has found applications in biotechnology, biomedicine, etc. One can cite the following as examples of current or potential applications. Cherry micelles containing core-encapsulated QDs are emerging as a new class of fluorescent probes for biomolecular and cellular imaging.[12,51] They effectively solved many problems encountered in utilization of QDs in biological environments, including water solubility enhancement, aggregation prevention, circulation time extension, and toxicity clearance, while retaining the unique optoelectronic properties of QDs.[12,51] Controlled clustering of magnetic NPs inside BCP aggregates results in high particle loading and a considerable increase in detection sensitivity in magnetic resonance imaging.[18,23a,40,44] The aggregates loaded with magnetic NPs and drugs can be directed to the drug-needing locations by magnetic fields.[23a,44] Drug release can be controlled through an oscillating magnetic field producing local hyperthermia in the magnetic particle loaded portion of the aggregates, which requires the precise localization of NPs in the corresponding parts of the aggregates, for example, micelle cores[23a] or vesicle walls.[44] Precise control of interparticle spacing of NPs within BCP aggregates, for example, cylindrical micelles, would be useful in sensors or nonlinear optics, taking advantage of the plasmonic coupling effect of NPs.[16,34]

BCP aggregates with precisely localized NPs are evolving toward novel structures, properties, and functions for applications. The challenges involve exploration of new controllable assembly strategies, deep understanding of structure–property relationships to predict the performance of a given structure, and creation of systematic theories.[4] With these advances, precise localization of NPs in BCP aggregates of controllable morphologies holds promise for fabrication of functional materials with tailored structures, functionalities, and applications.

The authors thank the Natural Science and Engineering Research Council of Canada (NSERC) for financial support.

BIOGRAPHICAL INFORMATION

Yiyong Mai received his Ph.D. from Shanghai Jiao Tong University in 2007 under the cosupervision of Professors Deyue Yan and Yongfeng Zhou. He is a Research Associate with Professor Adi Eisenberg at McGill University. His present research interests involve synthesis and self-assembly of polymers and exploration of polymer aggregates containing inorganic nanoparticles and their potential applications.

Adi Eisenberg received his Ph.D. from Princeton University in 1960 under the direction of A. V. Tobolsky. He has been a professor at McGill University since 1967, where he is currently Otto Maass Emeritus Professor. He is a fellow of the Royal Society of Canada and of the American Physical Society. His research interests include, among others, the exploration of self-assembled block copolymer aggregates and their potential applications.

FOOTNOTES

*Corresponding author. E-mail: adi.eisenberg@mcgill.ca.
The authors declare no competing financial interest.

REFERENCES

1 Moffitt, M.; Khougaz, K.; Eisenberg, A. Micellization of Ionic Block Copolymers. *Acc. Chem. Res.* **1996**, *29*, 95–102.
2 Förster, S.; Antonietti, M. Amphiphilic Block Copolymers in Structure-Controlled Nanomaterial Hybrids. *Adv. Mater.* **1998**, *10*, 195–217.
3 Bockstaller, M. R.; Mickiewicz, R. A.; Thomas, E. L. Block Copolymer Nanocomposites: Perspectives for Tailored Functional Materials. *Adv. Mater.* **2005**, *17*, 1331–1349.
4 Balazs, A. C.; Emrick, T.; Russell, T. P. Nanoparticle Polymer Composites: Where Two Small Worlds Meet. *Science* **2006**, *314*, 1107–1110.
5 Fahmi, A.; Pietsch, T.; Mendoza, C.; Cheval, N. Functional Hybrid Materials. *Mater. Today* **2009**, *12*, 44–50.
6 Yuan, J.; Müller, A. H. E. One-Dimensional Organic-Inorganic Hybrid Nanomaterials. *Polymer* **2010**, *51*, 4015–4036.
7 (a) Mai, Y.; Eisenberg, A. Self-Assembly of Block Copolymers. *Chem. Soc. Rev.* DOI: 10.1039/c2cs35115c. (b) Discher, D. E.; Ahmed, F. Polymersomes. *Annu. Rev. Biomed. Eng.* **2006**, *8*, 323–341.
8 Brust, M.; Walker, M.; Bethell, D.; Schiffrin, D. J.; Whyman, R. Synthesis of Thiol-Derivatised Gold Nanoparticles in a Two-Phase Liquid-Liquid System. *J. Chem. Soc., Chem. Commun.* **1994**, 801–802.
9 Templeton, A. C.; Wuelfing, W. P.; Murray, R. W. Monolayer-Protected Cluster Molecules. *Acc. Chem. Res.* **2000**, *33*, 27–36.
10 Li, D.; He, Q.; Li, J. Smart Core/Shell Nanocomposites: Intelligent Polymers Modified Gold Nanoparticles. *Adv. Colloid Interface Sci.* **2009**, *149*, 28–38.
11 Chen, T.; Yang, M.; Wang, X.; Tan, L.; Chen, H. Controlled Assembly of Eccentrically Encapsulated Gold Nanoparticles. *J. Am. Chem. Soc.* **2008**, *130*, 11858–11859.
12 Gao, X.; Cui, Y.; Levenson, R. M.; Chung, L. W. K.; Nie, S. In Vivo Cancer Targeting and Imaging with Semiconductor Quantum Dots. *Nat. Biotechnol.* **2004**, *22*, 969–976.
13 Kang, Y.; Taton, T. A. Core/Shell Gold Nanoparticles by Self-Assembly and Crosslinking of Micellar, Block-Copolymer Shells. *Angew. Chem., Int. Ed.* **2005**, *44*, 409–412.
14 Kang, Y.; Taton, T. A. Controlling Shell Thickness in Core–Shell Gold Nanoparticles via Surface-Templated Adsorption of Block Copolymer Surfactants. *Macromolecules* **2005**, *38*, 6115–6121.
15 Chen, H.; Abraham, S.; Mendenhall, J.; Delamarre, S. C.; Smith, K.; Kim, I.; Batt, C. A. Encapsulation of Single Small Gold Nanoparticles by Diblock Copolymers. *ChemPhysChem* **2008**, *9*, 388–392.
16 Mai, Y.; Eisenberg, A. Controlled Incorporation of Particles into the Central Portion of Block Copolymer Rods and Micelles. *Macromolecules* **2011**, *44*, 3179–3183.
17 Frankamp, B. L.; Uzun, O.; Ilhan, F.; Boal, A. K.; Rotello, V. M. Recognition-Mediated Assembly of Nanoparticles into Micellar Structures with Diblock Copolymers. *J. Am. Chem. Soc.* **2002**, *124*, 892–893.
18 For example: (a) Euliss, L. E.; Grancharov, S. G.; O'Brien, S.; Deming, T. J.; Stucky, G. D.; Murray, C. B.; Held, G. A. Cooperative Assembly of Magnetic Nanoparticles and Block Copolypeptides in Aqueous Media. *Nano Lett.* **2003**, *3*, 1489–1493. (b) Berret, J. F.; Schonbeck, N.; Gazeau, F.; Kharrat, D. E.; Sandre, O.; Vacher, A.; Airiau, M. Controlled

Clustering of Superparamagnetic Nanoparticles Using Block Copolymers: Design of New Contrast Agents for Magnetic Resonance Imaging. *J. Am. Chem. Soc.* **2006**, *128*, 1755–1761.

19 Moffitt, M.; Vali, H.; Eisenberg, A. Spherical Assemblies of Semiconductor Nanoparticles in Water-Soluble Block Copolymer Aggregates. *Chem. Mater.* **1998**, *10*, 1021–1028.

20 Yusuf, H.; Kim, W. G.; Lee, D. H.; Guo, Y.; Moffitt, M. Size Control of Mesoscale Aqueous Assemblies of Quantum Dots and Block Copolymers. *Langmuir* **2007**, *23*, 868–878.

21 Duxin, N.; Liu, F.; Vali, H.; Eisenberg, A. Cadmium Sulphide Quantum Dots in Morphologically Tunable Triblock Copolymer Aggregates. *J. Am. Chem. Soc.* **2005**, *127*, 10063–10069.

22 Kim, B. S.; Qiu, J.; Wang, J.; Taton, T. A. Magnetomicelles: Composite Nanostructures from Magnetic Nanoparticles and Cross-Linked Amphiphilic Block Copolymers. *Nano Lett.* **2005**, *5*, 1987–1991.

23 For example: (a) Nasongkla, N.; Bey, E.; Ren, J.; Ai, H.; Khemtong, C.; Guthi, J. S.; Chin, S. F.; Sherry, A. D.; Boothman, D. A.; Gao, J. Multifunctional Polymeric Micelles as Cancer-Targeted, MRI-Ultrasensitive Drug Delivery Systems. *Nano Lett.* **2006**, *6*, 2427–2430. (b) Gindy, M. E.; Panagiotopoulos, A. Z.; Prud'homme, R. K. Composite Block Copolymer Stabilized Nanoparticles: Simultaneous Encapsulation of Organic Actives and Inorganic Nanostructures. *Langmuir* **2008**, *24*, 83–90.

24 Zhang, L.; Lin, J.; Lin, S. Self-Assembly Behavior of Amphiphilic Block Copolymer/Nanoparticle Mixture in Dilute Solution Studied by Self-Consistent-Field Theory/Density Functional Theory. *Macromolecules* **2007**, *40*, 5582–5592.

25 Sanchez-Gaytan, B. L.; Cui, W. H.; Kim, Y. J.; Mendez-Polanco, M. A.; Duncan, T. V.; Fryd, M.; Wayland, B. B.; Park, S. J. Interfacial Assembly of Nanoparticles in Discrete Block-Copolymer Aggregates. *Angew. Chem., Int. Ed.* **2007**, *46*, 9235–9238.

26 Sanchez-Gaytan, B. L.; Li, S.; Kamps, A. C.; Hickey, R. J.; Clarke, N.; Fryd, M.; Wayland, B. B.; Park, S. J. Controlling the Radial Position of Nanoparticles in Amphiphilic Block-Copolymer Assemblies. *J. Phys. Chem. C* **2011**, *115*, 7836–7842.

27 Azzam, T.; Bronstein, L.; Eisenberg, A. Water-Soluble Surface-Anchored Gold and Palladium Nanoparticles Stabilized by Exchange of Low Molecular Weight Ligands with Biamphiphilic Triblock Copolymers. *Langmuir* **2008**, *24*, 6521–6529.

28 Guo, Y.; Harirchian-Saei, S.; Izumi, C. M. S.; Moffitt, M. Block Copolymer Mimetic Self-Assembly of Inorganic Nanoparticles. *ACS Nano* **2011**, *5*, 3309–3318.

29 Wang, M.; Kumar, S.; Lee, A.; Felorzabihi, N.; Shen, L.; Zhao, F.; Froimowicz, P.; Scholes, G. D.; Winnik, M. A. Nanoscale Co-organization of Quantum Dots and Conjugated Polymers Using Polymeric Micelles as Templates. *J. Am. Chem. Soc.* **2008**, *130*, 9481–9491.

30 Bertin, P. A.; Gibbs, J. M.; Shen, C. K.; Thaxton, C. S.; Russin, W. A.; Mirkin, C. A.; Nguyen, S. T. Multifunctional Polymeric Nanoparticles from Diverse Bioactive Agents. *J. Am. Chem. Soc.* **2006**, *128*, 4168–4169.

31 Zhu, J.; Hayward, R. C. Spontaneous Generation of Amphiphilic Block Copolymer Micelles with Multiple Morphologies through Interfacial Instabilities. *J. Am. Chem. Soc.* **2008**, *130*, 7496–7502.

32 Li, Z.; Sai, H.; Warren, S. C.; Kamperman, M.; Arora, H.; Gruner, S. M.; Wiesner, U. Metal Nanoparticle-Block Copolymer Composite Assembly and Disassembly. *Chem. Mater.* **2009**, *21*, 5578–5584.

33 Yang, S.; Wang, C.; Chen, S. Interface-Directed Assembly of One-Dimensional Ordered Architecture from Quantum Dots Guest and Polymer Host. *J. Am. Chem. Soc.* **2011**, *133*, 8412–8415.

34 Li, W.; Liu, S.; Deng, R.; Zhu, J. Encapsulation of Nanoparticles in Block Copolymer Micellar Aggregates by Directed Supramolecular Assembly. *Angew. Chem., Int. Ed.* **2011**, *50*, 5865–5868.

35 Zubarev, E. R.; Xu, J.; Sayyad, A.; Gibson, J. D. Amphiphilicity-Driven Organization of Nanoparticles into Discrete Assemblies. *J. Am. Chem. Soc.* **2006**, *128*, 15098–15099.

36 Wang, M.; Zhang, M.; Li, J.; Kumar, S.; Walker, G. C.; Scholes, G. D.; Winnik, M. A. Self-Assembly of Colloidal Quantum Dots on the Scaffold of Triblock Copolymer Micelles. *ACS Appl. Mater. Interfaces* **2010**, *2*, 3160–3169.

37 Wang, H.; Lin, W.; Fritz, K. P.; Scholes, G. D.; Winnik, M. A.; Manners, I. Cylindrical Block Co-Micelles with Spatially Selective Functionalization by Nanoparticles. *J. Am. Chem. Soc.* **2007**, *129*, 12924–12925.

38 Fresnais, J.; Berret, J. F.; Frka-Petesic, B.; Sandre, O.; Perzynski, R. Electrostatic Co-Assembly of Iron Oxide Nanoparticles and Polymers: Towards the Generation of Highly Persistent Superparamagnetic Nanorods. *Adv. Mater.* **2008**, *20*, 3877–3881.

39 Cui, H.; Chen, Z.; Zhong, S.; Wooley, K. L.; Pochan, D. J. Block Copolymer Assembly via Kinetic Control. *Science* **2007**, *317*, 647–650.

40 Lecommandoux, S.; Sandre, O.; Chécot, F.; Rodriguez-Hernandez, J.; Perzynski, R. Magnetic Nanocomposite Micelles and Vesicles. *Adv. Mater.* **2005**, *17*, 712–718.

41 Binder, W. H.; Sachsenhofer, R.; Farnika, D.; Blaasb, D. Guiding the Location of Nanoparticles into Vesicular Structures: A Morphological Study. *Phys. Chem. Chem. Phys.* **2007**, *9*, 6435–6441.

42 Krack, M.; Hohenberg, H.; Kornowski, A.; Lindner, P.; Weller, H.; Förster, S. Nanoparticle-Loaded Magnetophoretic Vesicles. *J. Am. Chem. Soc.* **2008**, *130*, 7315–7320.

43 Mueller, W.; Koynov, K.; Fischer, K.; Hartmann, S.; Pierrat, S.; Basché, T.; Maskos, M. Hydrophobic Shell Loading of PB-b-PEO Vesicles. *Macromolecules* **2009**, *42*, 357–361.

44 Sanson, C.; Diou, O.; Thévenot, J.; Ibarboure, E.; Soum, A.; Brûlet, A.; Miraux, S.; Thiaudière, E.; Tan, S.; Brisson, A.; Dupuis, V.; Sandre, O.; Lecommandoux, S. Doxorubicin Loaded Magnetic Polymersomes: Theranostic Nanocarriers for MR Imaging and Magneto-Chemotherapy. *ACS Nano* **2011**, *5*, 1122–1140.

45 Mai, Y.; Eisenberg, A. Controlled Incorporation of Particles into the Central Portion of Vesicle Walls. *J. Am. Chem. Soc.* **2010**, *132*, 10078–10084.

46 Hickey, R. J.; Haynes, A. S.; Kikkawa, J. M.; Park, S. J. Controlling the Self-Assembly Structure of Magnetic Nanoparticles Amphiphilic Block-Copolymers: From Micelles to Vesicles. *J. Am. Chem. Soc.* **2011**, *133*, 1517–1525.

47 Nikolic, M. S.; Olsson, C.; Salcher, A.; Kornowski, A.; Rank, A.; Schubert, R.; Frömsdorf, A.; Weller, H.; Förster, S. Micelle and Vesicle Formation of Amphiphilic Nanoparticles. *Angew. Chem., Int. Ed.* **2009**, *48*, 2752–2754.

48 Wang, M.; Zhang, M.; Siegers, C.; Scholes, G. D.; Winnik, M. A. Polymer Vesicles as Robust Scaffolds for the Directed Assembly of Highly Crystalline Nanocrystals. *Langmuir* **2009**, *25*, 13703–13711.

49 Opsteen, J. A.; Brinkhuis, R. P.; Teeuwen, R. L. M.; Löwik, D. W. P. M.; van Hest, J. C. M. "Clickable" Polymersomes. *Chem. Commun.* **2007**, 3136–3138.

50 Hou, G.; Zhu, L.; Chen, D.; Jiang, M. Core−Shell Reversion of Hybrid Polymeric Micelles Containing Gold Nanoparticles in the Core. *Macromolecules* **2007**, *40*, 2134–2140.

51 Maysinger, D.; Lovrić, J.; Eisenberg, A.; Savić, R. Fate of Micelles and Quantum Dots in Cells. *Eur. J. Pharm. Biopharm.* **2007**, *65*, 270–281.